MISSOURI S&T

Missouri University of Science and Technology

Scholars' Mine

Physics Faculty Research & Creative Works

Physics

01 Apr 2009

Role of Elastic Projectile-Electron Scattering in Double Ionization of Helium by Fast Proton Impact

Michael Schulz
Missouri University of Science and Technology, schulz@mst.edu

M. F. Ciappina

T. Kirchner

Daniel Fischer
Missouri University of Science and Technology, fischerda@mst.edu

et. al. For a complete list of authors, see *https://scholarsmine.mst.edu/phys_facwork/387*

Follow this and additional works at: https://scholarsmine.mst.edu/phys_facwork

Part of the Physics Commons

Recommended Citation

Role of elastic projectile-electron scattering in double ionization of helium by fast proton impact

M. Schulz,[1] M. F. Ciappina,[2] T. Kirchner,[3] D. Fischer,[4,5] R. Moshammer,[4] and J. Ullrich[4]

[1]*Department of Physics and Laboratory for Atomic, Molecular, and Optical Research, Missouri University of Science and Technology, Rolla, Missouri 65409, USA*

[2]*Institute of High Performance Computing, 1 Fusionopolis Way, #16-16 Connexis, 138632 Singapore, Singapore*

[3]*Institut für Theoretische Physik, TU Clausthal, Leibnizstr. 10, 38678 Clausthal-Zellerfeld, Germany*

[4]*Max-Planck-Institut für Kernphysik, Saupfercheckweg 1, 69117 Heidelberg, Germany*

[5]*Extreme Matter Institute EMMI, GSI Helmholtzzentrum für Schwerionenforschung GmbH, Planckstraße 1, 64291 Darmstadt, Germany*

We present a systematic study of atomic four-body fragmentation dynamics. To this end we have measured a variety of multiple differential double ionization cross sections for 6 MeV p+He collisions. The data are compared to a first-order calculation with correlated electrons and to a simulation representing a second-order process, with some experimental results seemingly in favor of the first, others in agreement with the second approach. This apparent conflict can be resolved by accounting for elastic scattering between the projectile and one electron already promoted to the continuum through electron-electron correlation in the first-order process.

PACS number(s): 34.50.Fa, 34.10.+x

I. INTRODUCTION

One of the most fundamental and yet unsolved challenges in physics is the time-dependent quantum few-body problem. The essence of it is that the Schrödinger equation is not solvable in closed form for more than two mutually interacting particles even if the underlying forces are precisely known. In order to advance our understanding of correlated few-body quantum dynamics inelastic reactions in atomic collisions have been studied extensively, especially exploring various prototypical three-body break-up processes (e.g., [1,2]).

Two-electron dynamics in atomic collisions, i.e., reactions in which two electrons undergo a transition, have also gained considerable interest because electron-electron correlations can play a very important role (e.g., [3–9]). Perhaps the simplest process for which dynamic correlations can be studied is double ionization (DI) of helium by single photon impact (e.g., [6,10–12]). Here, a good overall description has emerged and the basic features in measured cross sections can to a large extent be understood in terms of the dipole-selection rules in combination with the Coulomb repulsion between the electrons in the continuum [13,14].

DI by charged-particle impact, a four-body break-up process, instead is much more complex than photon impact because the transition of the target electrons evolves in a two-center potential generated by the target nucleus and the projectile. Furthermore, charged particles, in contrast to photons, can transfer a significant momentum to the target. As a result, the reaction dynamics of DI by charged-particle impact is much less understood than for photon impact (e.g., [7]). Therefore, in spite of a rich literature on this topic, experimental (e.g., [7,15–18]) and theoretical (e.g., [19–21]) studies on DI are still a very active field.

DI induced by charged-particle impact is often analyzed in terms of a correlated first-order mechanism (labeled two step—with one projectile-electron interaction or TS-1) and a higher-order mechanism (labeled two step—with two projectile-electron interactions or TS-2), where the latter

does not require the presence of electron-electron correlations [22]. In TS-1 the projectile only ejects one of the target electrons directly; the second electron is ejected through electron-electron correlation.[1] In TS-2, in contrast, both electrons are ejected by two independent interactions with the projectile. It is plausible to assume that with increasing projectile energy the relative importance of TS-1 increases because the perturbation and, thus, the second-order amplitude become smaller or, in an intuitive picture, it becomes less likely for two close encounters of the projectile with both electrons to occur at shorter collision times. Indeed, indications that at large projectile energies TS-1 contributions are significantly larger than those from TS-2 were found in measured DI to single ionization (SI) ratios [3]. Later, this was further supported by experimental fully differential cross sections (FDCSs) for fast electron impact [7,15]. Furthermore, nearly fully differential data for proton impact suggested that for ion-impact TS-2 contributions are even less important than for electron impact [16].

It was therefore quite surprising when we recently observed features in DI data for fast proton impact, which seemed to suggest a very important role of TS-2 [18]. There, four-particle Dalitz (4-D) plots were analyzed, a very new and powerful tool to study the collision dynamics in four-body fragmentation processes [23]. In a 4-D plot the momentum balance among all four collision fragments is represented simultaneously in a single spectrum using a tetrahedral coordinate system. Surprisingly, this four-particle momentum distribution (as well as other spectra) was much better reproduced by a TS-2 simulation than by a TS-1 calculation [18]. A puzzling conflict between earlier studies and these very recent results seemed to exist.

In this paper, we demonstrate that this apparent conflict can be resolved if elastic scattering between the projectile

---

[1]Sometimes, two mechanisms for the ejection of the second electron through electron-electron correlation are distinguished: ejection through a binary interaction with the first electron; ejection due to a sudden change in the effective potential after the removal of the first electron (so-called shake-off process).

and one of the electrons, predominantly ejected in a TS-1 process, is accounted for. Nevertheless, as far as the four-particle momentum balance presented in a 4-D plot is concerned, independent interactions between the projectile and both electrons do occur and are important for a detailed understanding of the dynamics. However, only one of these interactions is directly responsible for the ejection of the respective electron such that the "additional" interaction with the electron may not be visible in all measured spectra. Rather, it merely adds momentum to one (or both) electron already ejected in a TS-1 process. Therefore, our present results are consistent both with a strong role of TS-1 and significant momentum transfer from the projectile to both electrons observed in the recently reported 4-D plots. Furthermore, we demonstrate that other experimental data, like, e.g., multiple differential cross sections as a function of both electron ejection angles, are also reasonably well described by such a modified TS-1 model.

II. EXPERIMENT

The experimental method has been described in detail previously [18,24]. In short, a well-collimated 6 MeV proton beam was intersected with a very cold ($T \approx 1 - 2$ K) atomic helium beam from a supersonic jet. The ejected electrons and residual recoil ions produced in the collision were extracted by a weak electric field ($U \approx 2.3$ V/cm) and detected by two-dimensional position-sensitive channel-plate detectors. The electron detector was equipped with a delay line anode and could thus be operated in multihit mode. The essence of this operation is that both electrons ejected in a DI event can be detected simultaneously with a single detector. The recoil ions and both electrons were fully momentum analyzed using a standard COLTRIMS apparatus [24]. The momentum transfer $\mathbf{q}$ from the projectile to the target atom is then readily determined by momentum conservation: $\mathbf{q} = \mathbf{p}_{rec} + \mathbf{p}_1 + \mathbf{p}_2$, where $\mathbf{p}_{rec}$ is the recoil-ion momentum and $\mathbf{p}_1$ and $\mathbf{p}_2$ are the electron momenta.

The momentum resolutions depend on the momenta themselves and, therefore, averaged values are provided. In the longitudinal (z) direction they are ± 0.075 and ± 0.005 a.u. for the recoil ion and for the electrons, respectively. In the direction of the jet expansion (y direction), the corresponding numbers are ± 0.25 and ± 0.1 a.u., and for the x direction ± 0.1 a.u. for both the recoil ion and the electrons. Since the momentum resolution of the electrons is small compared to that of the recoil ion, the momentum transfer resolution is essentially the same as for the recoil ions.

III. THEORETICAL TS-1 MODEL AND TS-2 SIMULATION

The theoretical TS-1 model and a simulation of the contributions from TS-2, based on theoretical single ionization cross sections, have also been described in detail previously [18] and only the salient points will be repeated here. FDCSs for the TS-1 process were calculated within the first Born approximation (FBA). Radial correlation is accounted for in the initial state and in the final state electron-electron corre-

lation is treated in terms of the Gamov factor using dynamically screened electron charges [19,25]. For the TS-2 simulation FDCSs for single ionization of He and of He$^+$ were calculated also within the FBA and convoluted with each other.

Based on the theoretical FDCS an event file using a Monte Carlo simulation was generated following the method of Dürr *et al.* [26]. The event file contains all three momentum components of each electron and the x component of $\mathbf{q}$ for approximately 2×10^6 DI events. We used a coordinate system in which the x axis coincides with the transverse component of $\mathbf{q}$ such that $q_y = 0$ for all events. The z component q_z is readily determined by the sum energy of both electrons: $q_z = (\Sigma E_e + I)/v_0$, where I is the ionization potential and v_0 is the initial projectile speed. In the case of the TS-2 simulation the event file contains q_x for each single ionization event separately. For one of the ionization events the direction of $\mathbf{q}$ in the transverse (x, y) plane was randomized because for two independent single ionization events the relative orientation between the scattering planes is completely random. The total momentum transfer for TS-2 is then obtained from the sum of the single ionization momentum transfers. The final-state repulsion between the electrons was accounted for by the same Gamov factor as in the TS-1 calculation.

Finally, the TS-1 calculation and the TS-2 simulation were convoluted with the experimental resolution as described by Dürr *et al.* [26] and with classical elastic scattering between the projectile and the He nucleus, which is not accounted for by the FBA, following the method of Schulz *et al.* [27]. In case of the TS-2 simulation projectile scattering from both electrons is accounted for by the FBA so that for elastic scattering of the projectile from the nucleus the unscreened charge of 2 was used. In the TS-1 calculation, on the other hand, the projectile only scatters from one electron. To describe the projectile-nucleus scattering we therefore used a variable screened charge corresponding to a Hartree-Fock potential of a proton in the field of a He$^+$ ion [27]. For test purposes we also performed a calculation for $Q = 2$ and found no significant difference to the Hartree-Fock charge.

From the momentum components obtained from this procedure any other kinematic quantity, such as ejection angles or electron energies, can easily be calculated. Any cross section that can be extracted from the experimental data can also be generated from the theoretical event files by sorting these quantities in histograms and using appropriate conditions exactly the same way as in the data analysis.

IV. RESULTS AND DISCUSSION

Before revisiting the 4-D plots we will first present data, which have not been analyzed yet in terms of our theoretical TS-1 model and the TS-2 simulation. First, we discuss data, which at first glance seem to suggest, like the 4-D plots, a strong role of TS-2. We will then analyze data, which suggest a dominant role of TS-1. Finally, we will demonstrate that the resulting apparent conflict can be resolved by accounting for elastic projectile-electron scattering.

In Fig. 1 a triple differential angular distribution (TDAD) of the sum momentum of both ejected electrons $\mathbf{P}_{elec} = \mathbf{p}_1$
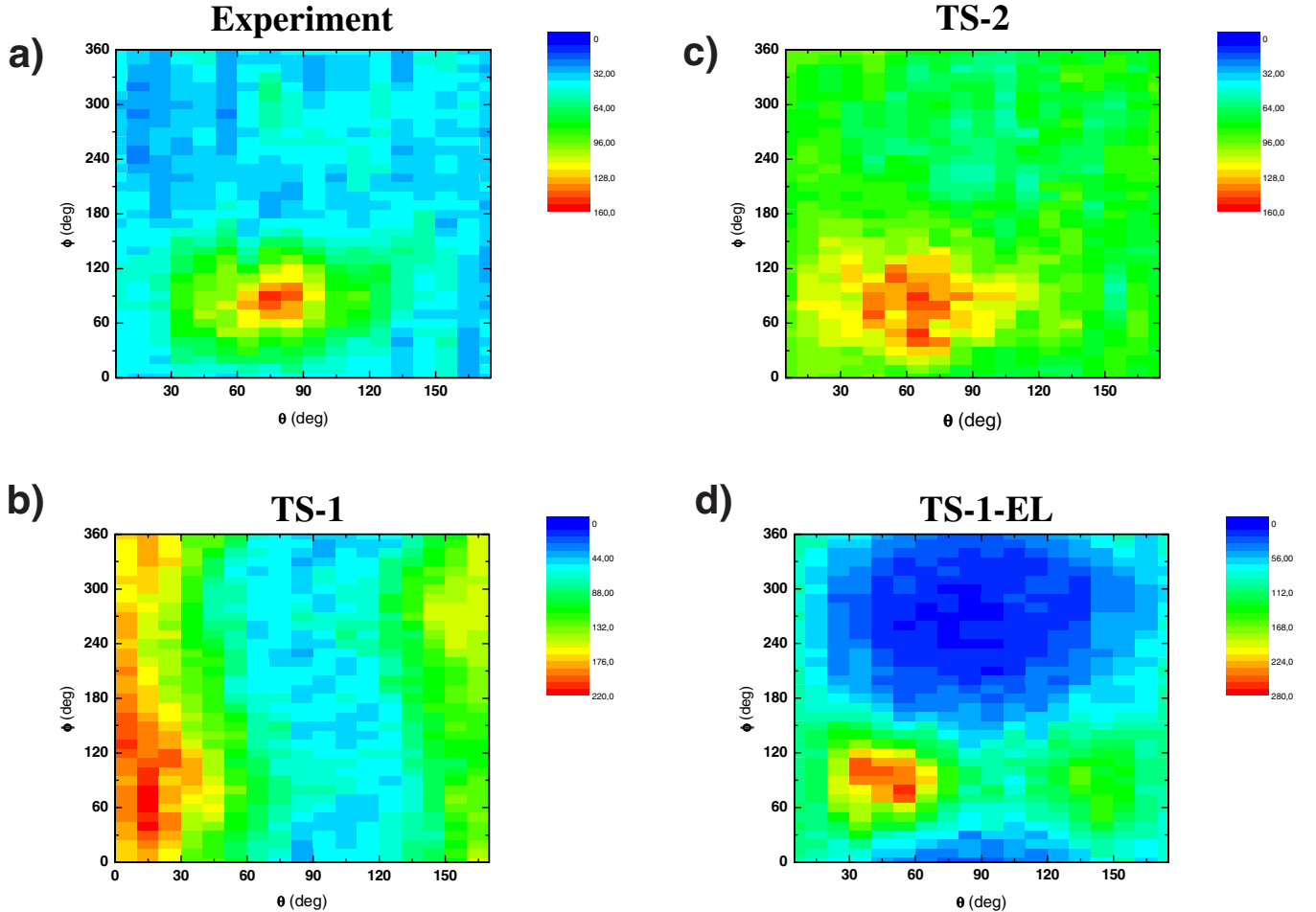
FIG. 1. (Color online) Triple differential angular distribution of the sum momentum of both ejected electrons $\mathbf{P}_{\text{elec}}$. The momentum transfer is fixed at $q=1.1\pm0.3$ a.u. and the electron sum energy at 11 ± 3 eV. The azimuthal angle φ is plotted on the vertical axis and the polar angle θ on the horizontal axis. $\varphi=90°$ corresponds to the semiplane containing $\mathbf{q}$ and the initial projectile momentum $\mathbf{p}_0$ and $\varphi=270°$ corresponds to the semiplane containing $-\mathbf{q}$ and $\mathbf{p}_0$. (a) Experimental data; (b) TS-1 calculation; (c) TS-2 simulation; and (d) TS-1-EL calculation (see text).

$+\mathbf{p}_2$ is plotted. Here, q is fixed at 1.1 ± 0.3 a.u. and ΣE_e at 11 ± 3 eV. The experimental data [panel (a)] have been published earlier [28]. The TS-1 calculation and the TS-2 simulation are shown in panels (b) and (c), respectively [for panel (d), see below]. The horizontal axis represents the polar angle Θ, measured relative to the projectile beam direction, and the vertical axis is the azimuthal angle ϕ of $\mathbf{P}_{\text{elec}}$. $\phi=90°$ represents the semiplane containing the initial projectile momentum $\mathbf{p}_0$ and $\mathbf{q}$. Therefore, the well-known binary peak, which occurs in the direction of $\mathbf{q}$ in the FBA, is expected in this semiplane. Likewise, $\phi=270°$ corresponds to the semiplane containing $\mathbf{p}_0$ and $-\mathbf{q}$, in which the recoil peak is expected.

In the experimental data indeed a pronounced binary peak is observed in the direction of $\mathbf{q}$, while the recoil peak is barely visible. It is striking, however, that the TS-1 calculation, which is based on the FBA, does not show a peak at all in the direction of $\mathbf{q}$ but rather a strong maximum is found in the forward direction (i.e., near $0°$). This apparent violation of the symmetry of the cross sections about $\mathbf{q}$, which is strictly required in the unconvoluted FBA, is due to the convolution with the experimental resolution. The steep dependence of the cross sections on q predicted by the FBA in combination with the large double ionization potential of $I=79$ eV makes the TS-1 calculation extremely sensitive to the convolution. Thus, the large I corresponds to a relatively large longitudinal momentum transfer component, as seen from the equation above. Therefore, at small q's, which then contribute significantly to larger q due to the convolution with the resolution, $\mathbf{q}$ is strongly pointing in the forward direction. In single ionization, in contrast, where the ionization potential is much smaller (24.6 eV), the FBA is much less sensitive to this effect [26]. In the TS-1 calculation without any convolution the binary peak is indeed found in the direction of $\mathbf{q}$, however, its intensity is then much too small compared to experiment. In fact, the statistics (originating from the Monte Carlo procedure) in the TS-1 calculation for $q=1.1$ a.u. is so poor that the binary peak can hardly be recognized (at small q, however, it is clearly seen in the direction of $\mathbf{q}$). The large shift of the binary peak in the forward direction, which is obviously not observed in the data, is a manifestation of the FBA predicting a much too steep q dependence of the DI cross sections, which we reported earlier already [18].
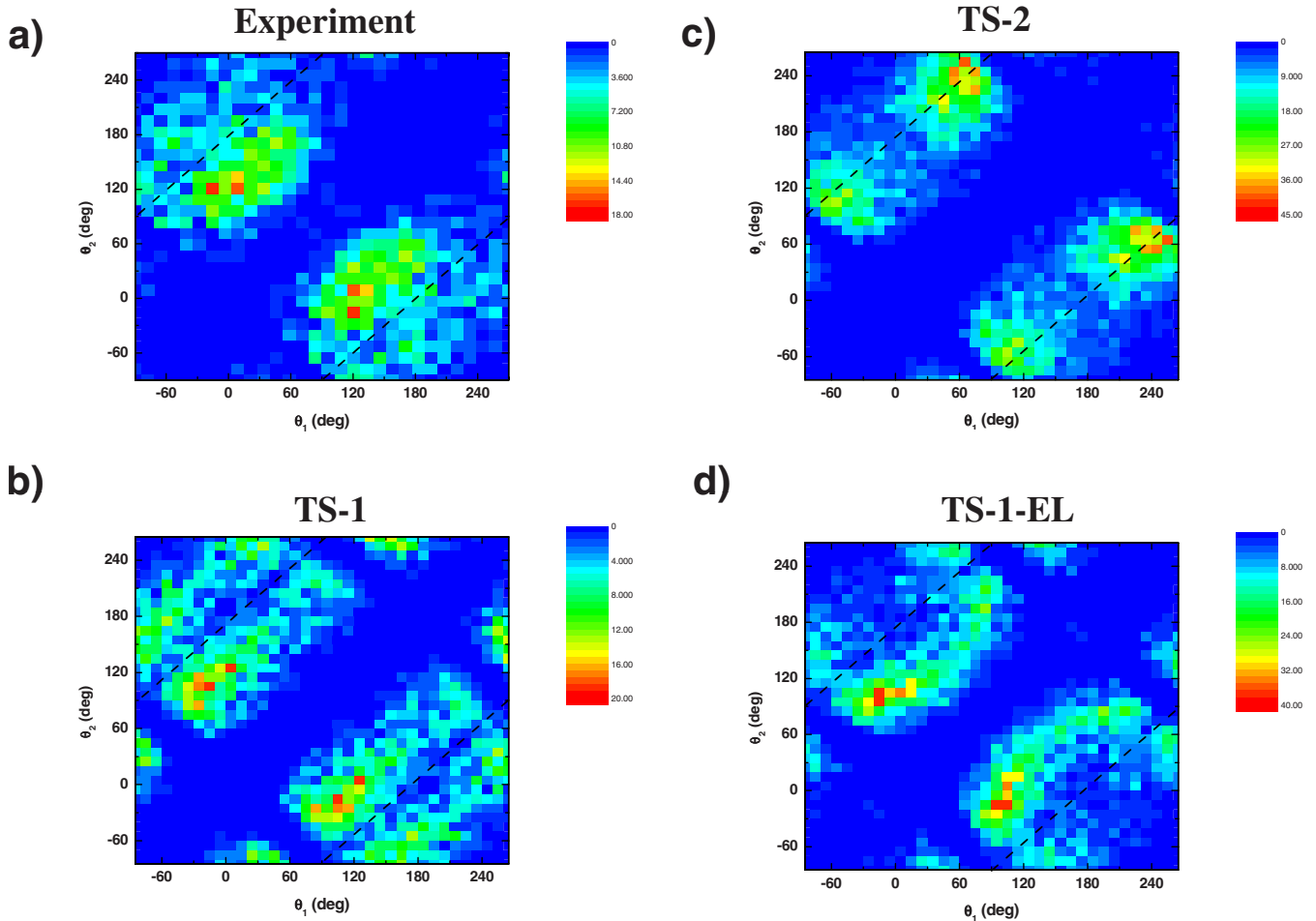
FIG. 2. (Color online) Fourfold differential cross sections as a function of the polar angles of both ejected electrons. Only electrons of equal energy (within 2.5 eV) ejected into the scattering plane are selected. The momentum transfer is fixed at $q = 1.1 \pm 0.3$ a.u. Panels (a)–(d): same as in Fig. 1.

With or without convolution, the TS-1 calculation is in very poor agreement with the experimental data (either in shape or in intensity). Some discrepancies are found in the TS-2 simulation as well. The binary peak is still shifted in the forward direction; however, this shift is much smaller (about $10° - 15°$) than in the TS-1 results. Furthermore, it appears to be somewhat broader than in the data. Nevertheless, the TS-2 simulation is clearly in much better agreement with the data than the TS-1 calculation. It should also be noted that the TS-2 result is hardly affected by the convolution with the resolution because it reproduces the q dependence of the cross sections much better than the TS-1 calculation. These observations are thus consistent with our earlier findings from the analysis of 4-D plots [18], which strongly suggest that the projectile transfers a significant momentum directly to both electrons.

We now turn to fourfold differential cross sections (4DCSs) for electrons of equal energy ejected into the scattering plane (defined by $\mathbf{p}_0$ and $\mathbf{q}$) at fixed q as a function of the two polar electron ejection angles. Experimental data for these cross sections have been reported earlier [16] and are shown in panel (a) of Fig. 2 for $q = 1.1 \pm 0.3$ a.u. "Equal electron energies" are defined such that the difference between the individual electron energies is smaller than 2.5 eV.

Again, the TS-1 calculation and the TS-2 simulation are shown in panels (b) and (c), respectively.

Similarly to the TDAD again both the TS-1 calculation and the TS-2 simulation show some discrepancies to the measured 4DCS. However, this time the TS-1 calculation clearly fares better than the TS-2 simulation. The binary peak in the data at an angle combination of about $(0°, 120°)$ is more or less reproduced by TS-1. In contrast, in the TS-2 simulation two peak structures are observed at angle combinations of $(60°, 240°)$ and $(-60°, 120°)$ which are not present at all in the data. Most importantly, the characteristic signatures of the dipole-selection rules [14] are completely missing in the TS-2 simulation. These rules state that back-to-back emission of two electrons of equal energy originating from an s^2 state is not allowed by an electric dipole transition. In the spectra of Fig. 2 this prohibition should suppress angle combinations indicated by the dashed lines. Indeed, in the TS-1 calculation a reduced intensity along these lines can clearly be seen. The TS-2 simulation, in contrast, even yields pronounced maxima. The experimental data clearly favor TS-1: the main maxima are displaced diagonally from the dipole-selection-rule depleted lines toward the center of the spectrum and even a significant suppression along these lines can be seen.

A dominance of electric dipole transitions in the TS-1 mechanism is expected since it is a first-order process. The TS-2 contribution, on the other hand, entails two independent electron transitions, of which each is dominated by electric dipole transitions as well. Because of angular momentum conservation and helicity considerations one would then expect that TS-2 leads mostly to final two-electron states with an angular momentum of 0 or 2, i.e., the dipole-selection rules should not hold for TS-2. At the same time the Coulomb repulsion between the electrons, especially for equal energies, should even enhance the 4DCS for back-to-back emission. Therefore the presence of the dipole-selection rule depleted lines in the experimental data is a strong indication that TS-2 does not significantly contribute to DI, in accord with earlier studies (e.g., [3]).

As a preliminary summary, the TDAD and the 4-D plots reported earlier [18] suggest that the projectile transfers significant momentum to both electrons directly. On the other hand, the 4DCS strongly supports earlier conclusions that at these large projectile energies DI is dominated by TS-1. The question to be answered is how these two observations, which at first glance may seem incompatible with each other, can be reconciled. To consider one possibility we point out that a significant momentum transfer from the projectile to both electrons does not necessarily imply that both electrons are ejected by direct interactions with the projectile. Rather, the projectile may elastically scatter from one (or both) electron(s) already ejected through electron-electron correlation in a TS-1 process. We label this process TS-1-EL, although in some sense this might be somewhat misleading. The first part of the label, TS-1, is appropriate in so far as only one electron is ejected by a direct interaction with the projectile and the second electron is ejected through electron-electron correlation, as in the standard TS-1 process. On the other hand TS-1 is usually viewed as a first-order process, while TS-1-EL is a second- (or higher) order process[2] because it involves two interactions of the projectile with both electrons. In that sense TS-1-EL has more resemblance with TS-2 and is perhaps best viewed as a hybrid between TS-1 and TS-2.

To investigate the role of the TS-1-EL process we have convoluted the TS-1 calculation with classical elastic projectile-electron scattering (in addition to the convolution with elastic projectile-target nucleus scattering and with the experimental resolution). We consider elastic scattering only from one electron since the interaction of the projectile with the other electron, the one which is ejected directly by the projectile, is accounted for by the FBA. Strictly speaking we cannot distinguish, of course, which electron got ejected directly by the projectile and which one through electron-electron correlation. Since on average the direct ejection requires a relatively close collision with the projectile we treat, somewhat arbitrarily, the slower electron as the one ejected by correlation and from which the projectile elastically scatters.

As a first step of the convolution the position distribution of the electron in the initial state $\Psi_i(r)$ with respect to the nucleus was simulated using a random generator such that the quantum mechanical distribution $|\Psi_i(r)|^2$ was modeled. Since the electron is slow compared to the projectile we assume that its position distribution does not differ significantly from the one in the ground state, which we approximate to be hydrogenic. The convolution with elastic projectile-target nucleus scattering, for which now a target nucleus charge of 2 is used instead of the Hartree-Fock charge, already entails a simulation of the distribution of the impact parameter with respect to the target nucleus b_n (for details, see [27]). From the initial position of the electron and b_n it is straightforward to calculate the impact parameter with respect to the electron b_e. Assuming classical Rutherford scattering for a $1/r$ potential the momentum transferred from the projectile to the electron q_e is then given by $q_e = 2/(b_e v_0)$ (in a.u.), which is added to the momentum transfer and to the electron momentum calculated with the FBA.

The classical treatment of elastic projectile-electron scattering entails approximations (as for elastic projectile-target nucleus scattering, see Ref. [27]), which should be kept in mind when comparing the result of this convolution to the data. First, TS-1 with and without elastic projectile-electron scattering is not treated coherently. Second, the above relation between q_e and b_e is not strictly valid because the impact parameter is not an observable quantity in quantum mechanics. On the other hand, this classical treatment has been successfully applied to projectile-target nucleus scattering in single ionization [27] and in double ionization [18].

First, we discuss the effect of the convolution with elastic projectile-electron scattering on the 4-D representation. In these spectra the relative squared momenta $\pi_i = p_i^2/\Sigma p_j^2$ are plotted, where p_j are the momenta of the four collision fragments (except for the projectile, for which the momentum transfer is used, instead). These π_i are presented in a tetrahedral coordinate system, where each plane represents one of the four particles. For a given data point a set of the four π_i is given by the distances of the data point to the four tetrahedron planes. More details regarding the methodology of 4-D representation can be found in Refs. [18,23].

In Fig. 3 4-D plots, in which the π_i were calculated only using the transverse component in the scattering plane for each particle, are shown. The experimental data [panel (a)], the TS-1 calculation [panel (b)], and the TS-2 simulation [panel (c)] were reported previously [18]. Binary interactions, for which the momenta of two particles are zero, so that the momentum exchange takes place only between the other two particles, occur at the intersection lines between adjacent tetrahedron planes. These intersection lines are labeled 1–6 in Fig. 3(a). To summarize the earlier results, the TS-1 calculation is in poor agreement with the experimental data. In particular, it predicts strong contributions near intersection lines 2 and 3 (representing binary momentum exchange between the He nucleus and one of the electrons), which are not seen at all in the data. Furthermore, binary interactions between the projectile and one of the electrons (intersection lines 4 and 5), and especially the region near the lower left corner of the tetrahedron (corresponding to large momentum transfer collisions), are significantly underesti-

---

[2]Although it should be noted that TS-1-EL also contains pure TS-1 contributions because classical elastic scattering allows for zero-angle deflection and, in fact, the Rutherford cross section maximizes there.
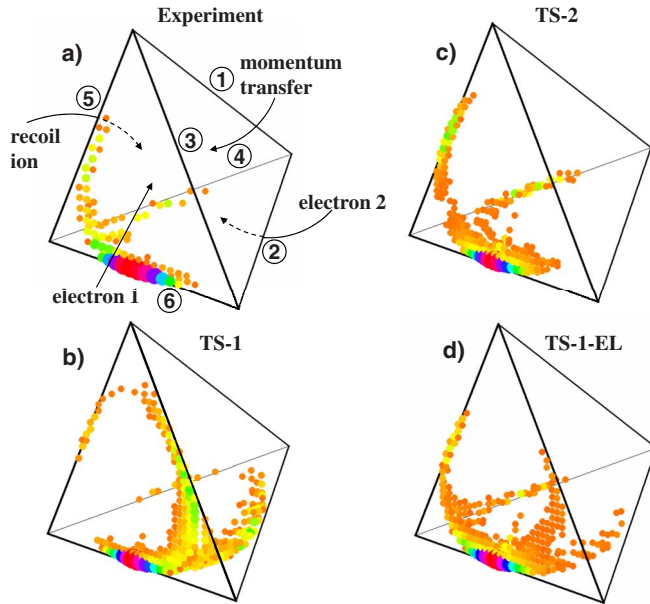
FIG. 3. (Color online) Four-particle Dalitz plots. The numbers label intersection lines between adjacent tetrahedral planes, where binary interactions between two particles occur. Panels (a)–(d): same as in Fig. 1.

mated by the TS-1 calculation. The TS-2 simulation, on the other hand, is in nice qualitative agreement with the measurement.

In panel (d) we present the TS-1-EL results. Undoubtedly, the agreement with the data is substantially improved compared to the TS-1 calculation. Although contributions from binary He nucleus–electron momentum exchange are still present, they are nevertheless strongly suppressed. Furthermore, the binary projectile-electron interactions and large momentum transfer collisions are now qualitatively reproduced. Small, but nonzero, TS-2 contributions can probably explain the remaining discrepancies near intersection lines 2 and 3. The similarity between the TS-1-EL calculation and the TS-2 simulation illustrates how delicate attempts to distinguish correlated from uncorrelated DI mechanisms from qualitative features in measured data can be.

A similar effect of elastic projectile-electron scattering is found in the TDAD in Fig. 1, where the TS-1-EL calculation is shown in panel (d). Here too, the significantly improved agreement with the data compared to the TS-1 calculation is quite obvious. The binary peak is strongly moved away from the forward direction and the calculation is much less sensitive to the experimental resolution. As far as the peak position is concerned the agreement with the data is not as good as for the TS-2 simulation. On the other hand, its width is even better reproduced by the TS-1-EL calculation both in φ and θ.

The apparent success of the convolution with elastic projectile-electron scattering is, of course, of no avail if it would lead at the same time to significantly worse agreement with the data in the 4DCS compared to the TS-1 calculation since here the latter fares much better than the TS-2 simulation. In particular, if the minima along the dipole-forbidden lines would be filled up, or even transformed into maxima,

like in the TS-2 simulation, the TS-1-EL model could immediately be discarded. In panel (d) of Fig. 2 we therefore compare the 4DCS calculated with the TS-1-EL model to the spectra of panels (a)–(c). In this case the effect of elastic projectile-electron scattering is rather weak. Most importantly a pronounced dipole line is still visible. Compared to the TS-1 calculation it is partly filled up, but this is, in fact, in accord with the data where the dipole line is even less pronounced. In this sense, the TS-1-EL calculation actually leads to a slightly improved agreement compared to the TS-1 calculation.

Overall, the convolution with elastic projectile-electron scattering significantly improves the agreement with the data whenever the TS-2 simulation fares better than the TS-1 calculation. At the same time, this convolution at least does not make the agreement worse (in fact, it seems to slightly improve it) in cases where the TS-1 calculation is in better agreement with the data than the TS-2 simulation. Elastic projectile-electron scattering therefore offers a possibility to reconcile the four-particle momentum balance and the TDAD on one hand (which suggest significant momentum transfer from the projectile to both electrons directly) with the 4DCS on the other hand (which suggest a dominance of the TS-1 process).

An important test of the role of TS-1-EL could be offered by a rigorous (which the present TS-2 simulation is not) higher-order calculation. Such a model would include all mechanisms discussed here. If the amplitudes were computed exactly (which, of course, is currently not possible), it should, in principle, correctly reproduce the relative importance of these contributions. On the other hand, in the case of single ionization it is known that perturbative approaches tend to underestimate elastic scattering between the projectile and the residual target ion [1,26,27]. One might suspect that in DI a similar problem could occur with regard to elastic projectile-electron scattering. Nevertheless, a rigorous higher-order calculation could shed more light on the role of the various DI mechanisms.

V. CONCLUSIONS

We have analyzed the four-particle momentum balance in double ionization of helium by fast proton impact using 4-D plots, TDADs of the sum momentum of the ejected electrons, and 4DCSs as a function of the polar ejection angles of the two electrons. Measured data were compared to a first-order calculation and a second-order simulation. In the first-order process (TS-1) one electron is ejected by a direct interaction with the projectile and the second electron by electron-electron correlation. In the second-order process, both electrons are ejected by two independent direct interactions with the projectile. While the 4-D plots and the TDAD suggest an important role of two independent direct projectile-electron interactions, the 4DCSs strongly suggest a dominance of the TS-1 process. At the same time the latter is expected to dominate on the basis of numerous experiments and calculations on total cross section ratios.

In this paper we demonstrated that one possibility of reconciling the observations in the 4-D plots, the TDAD, and in

the 4DCS is to account for elastic scattering between the projectile and the electron which is already lifted to the continuum in a TS-1 process through electron-electron correlation (which we assumed to be the slower electron). Incorporating this elastic scattering consistently on the basis and with the limitations of the classical approach leads to significantly improved agreement in spectra which are better described by TS-2 than by TS-1 and to at least as good agreement as TS-1 in spectra which are better described by TS-1 than by TS-2. In spite of the approximations associated with the classical treatment of elastic scattering, which render detailed quantitative comparisons uncertain, the systematic qualitative success of our model strongly suggests an important role of elastic projectile-electron scattering in double ionization.

The model proposed here may also settle a puzzle that resulted earlier from a comparison between measured total DI cross sections for ion and antiproton impact. On one hand the ion-impact data show a Z^2 dependence of the cross sections at large projectile energies (where Z is the projectile atomic number), which is a characteristic feature of a first-order process. On the other hand, clear differences between proton and antiproton data were observed [3]. In a perturbation expansion, such differences can only result from terms in the cross sections containing an odd-power Z dependence. Fischer *et al.* [16] suggested that a Z^4 term (representing second-order mechanisms) may for proton impact be canceled by a destructive Z^3 interference term between first-order and second-order terms, while for antiproton impact it gets enhanced by constructive interference. Contributions from TS-2 may be too weak for this explanation; however, TS-1-EL is also a higher-order process which could result in an interference term. In this paper we demonstrated that TS-1-EL contributions could be quite important and therefore resolve this puzzle. More sophisticated higher-order calculations are called for to investigate this point in more detail.

[1] M. Schulz, R. Moshammer, D. Fischer, H. Kollmus, D. H. Madison, S. Jones, and J. Ullrich, Nature (London) **422**, 48 (2003).

[2] T. N. Rescigno, M. Baertschy, W. A. Isaacs, and C. W. McCurdy, Science **286**, 2474 (1999).

[3] L. H. Andersen, P. Hvelplund, H. Knudsen, S. P. Møller, K. Elsener, K.-G. Rensfelt, and E. Uggerhøj, Phys. Rev. Lett. **57**, 2147 (1986).

[4] M. Schulz, E. Justiniano, R. Schuch, P. H. Mokler, and S. Reusch, Phys. Rev. Lett. **58**, 1734 (1987).

[5] W. T. Htwe, T. Vajnai, M. Barnhart, A. D. Gaus, and M. Schulz, Phys. Rev. Lett. **73**, 1348 (1994).

[6] J. C. Levin, D. W. Lindle, N. Keller, R. D. Miller, Y. Azuma, N. B. Mansour, H. G. Berry, and I. A. Sellin, Phys. Rev. Lett. **67**, 968 (1991).

[7] A. Dorn, A. Kheifets, C. D. Schröter, B. Najjari, C. Höhr, R. Moshammer, and J. Ullrich, Phys. Rev. Lett. **86**, 3755 (2001).

[8] S. Bellm, J. Lower, and K. Bartschat, Phys. Rev. Lett. **96**, 223201 (2006).

[9] M. Schulz, T. Vajnai, and J. A. Brand, Phys. Rev. A **75**, 022717 (2007).

[10] O. Schwarzkopf, B. Krässig, J. Elmiger, and V. Schmidt, Phys. Rev. Lett. **70**, 3008 (1993).

[11] P. Lablanquie, J. Mazeau, L. Andric, P. Selles, and A. Huetz, Phys. Rev. Lett. **74**, 2192 (1995).

[12] R. Dörner, J. M. Feagin, C. L. Cocke, H. Bräuning, O. Jagutzki, M. Jung, E. P. Kanter, H. Khemliche, S. Kravis, V. Mergel, M. H. Prior, H. Schmidt-Böcking, L. Spielberger, J. Ullrich, M. Unversagt, and T. Vogt, Phys. Rev. Lett. **77**, 1024 (1996).

[13] A. Huetz, P. Selles, D. Waymel, and J. Mazeau, J. Phys. B **24**, 1917 (1991).

[14] F. Maulbetsch and J. S. Briggs, J. Phys. B **28**, 551 (1995).

[15] I. Taouil, A. Lahmam-Bennani, A. Duguet, and L. Avaldi, Phys. Rev. Lett. **81**, 4600 (1998).

[16] D. Fischer, R. Moshammer, A. Dorn, J. R. Crespo Lopez-Urrutia, B. Feuerstein, C. Hohr, C. D. Schroter, S. Hagmann, H. Kollmus, R. Mann, B. Bapat, and J. Ullrich, Phys. Rev. Lett. **90**, 243201 (2003).

[17] M. Schulz, R. Moshammer, W. Schmitt, H. Kollmus, B. Feuerstein, R. Mann, S. Hagmann, and J. Ullrich, Phys. Rev. Lett. **84**, 863 (2000).

[18] M. F. Ciappina, M. Schulz, T. Kirchner, D. Fischer, R. Moshammer, and J. Ullrich, Phys. Rev. A **77**, 062706 (2008).

[19] L. Gulyás, A. Igarashi, and T. Kirchner, Phys. Rev. A **74**, 032713 (2006).

[20] M. Foster, J. Colgan, and M. S. Pindzola, J. Phys. B **41**, 111002 (2008).

[21] E. M. Lobanova, S. A. Sheinerman, and L. G. Gerchikov, J. Exp. Theor. Phys. **105**, 486 (2007).

[22] J. H. McGuire, *Electron Correlation Dynamics in Atomic Collisions* (Cambridge University Press, Cambridge, 1997).

[23] M. Schulz, D. Fischer, T. Ferger, R. Moshammer, and J. Ullrich, J. Phys. B **40**, 3091 (2007).

[24] R. Moshammer, M. Unverzagt, W. Schmitt, J. Ullrich, and H. Schmidt-Böcking, Nucl. Instrum. Methods Phys. Res. B **108**, 425 (1996).

[25] J. R. Götz, M. Walter, and J. S. Briggs, J. Phys. B **38**, 1569 (2005).

[26] M. Dürr, B. Najjari, M. Schulz, A. Dorn, R. Moshammer, A. B. Voitkiv, and J. Ullrich, Phys. Rev. A **75**, 062708 (2007).

[27] M. Schulz, M. Dürr, B. Najjari, R. Moshammer, and J. Ullrich, Phys. Rev. A **76**, 032712 (2007).

[28] D. Fischer, M. Schulz, R. Moshammer, and J. Ullrich, J. Phys. B **37**, 1103 (2004).